KSME

Springer

Journal of Mechanical Science and Technology 39 (0) 2025

Original Article
DOI 10.1007/s12206-025-0000-0

Keywords:
· Nanocomposites
· Multi-walled carbon nanotubes (MWCNTs)
· Graphene platelets (GPLs)
· Wind turbine blades
· Finite element structural analysis
· Comparative analysis

Correspondence to:
Jin-Rae Cho
jrcho@hongik.ac.kr

† This paper was recommended for publication in revised form by Associate Editor

Citation:
Kim, H. J., Cho, J.-R. (2025). Carbon nanotube- and graphene-reinforced composites: which is better for wind turbine blade applications?. Journal of Mechanical Science and Technology 39 (0) (2025) 0000~0000.
https://doi.org/10.1007/s12206-025-0000-0

Received Month 00th, 2025
Revised Month 00th, 2025
Accepted Month 00th, 2025

† Recommended by Editor
No-cheol Park

Carbon nanotube- and graphene-reinforced composites: which is better for wind turbine blade applications?

Hyeong Jin Kim[1] and Jin-Rae Cho[2]

[1]Department of Mechanical Engineering, University College London, London, WC1E 7JE, UK,
[2]Department of Naval Architecture and Ocean Engineering, Hongik University, Sejong 30016, Korea

Abstract Nanocomposites reinforced with carbon nanotubes (CNTs) or graphene-based materials have garnered increasing attention for improving the structural performance of engineering systems, owing to their exceptional mechanical properties. Accordingly, the mechanical behaviors and applicability of both nanocomposites have been intensively investigated, but the studies on both composites have been mostly investigated separately. In this context, this study intends to investigate which is better for wind turbine blade applications, where both lightweight and high-strength and high-durability are critical. The comparisons are made in terms of static bending and torsion, free vibration and fatigue life which are analyzed by finite element analyses. Finite element wind turbine models are generated based on the 61.5 m SNL reference design by Sandia National Laboratories, incorporated with the appropriate theories for deriving the effective material properties and evaluating the fatigue lives. The comparative numerical experiments are carried out for CNT- and graphene-reinforced wind turbine blades as well as the conventional glass fiber reinforced (GFRP) one. The numerical results reveal that the performance of conventional GFRP wind blade has been remarkably improved when GFRP was replaced with carbon-based nanocomposites. Between two nanocomposites, the graphene-reinforced composite is found to be better suited for wind turbine applications.

1. Introduction

The recent escalation in global energy demand, combined with the urgent need to mitigate climate change caused by greenhouse gas emissions, has led to growing interest in renewable energy technologies. Among available options, wind energy stands out as one of the most promising forms of future energy, alongside solar power, due to its minimal geographical constraints and potential for large scale power generation. As the wind energy sector continues to expand, efforts to increase their size for improved energy output have accelerated, introducing a series of engineering challenges such as higher structural loads, increased mass, and the demand for enhanced fatigue resistance. Notably, the blade has a direct impact on both the system's energy generation efficiency and structural reliability. To address these issues, various advanced materials have been investigated for their potential to improve strength and reduce weight, including basalt fiber composites [1, 2], carbon fiber composites [3], and bamboo-based natural fiber composites [4, 5].

Nanocomposites incorporating advanced nanomaterials have attracted substantial interest, particularly with the rapid progress in nanotechnology since the early 21st century. Compared to conventional composites, nanocomposites exhibit much shorter surface-to-surface interparticle distances and significantly larger interfacial areas of nanofillers at the same volume fraction, which contribute to their superior strength to weight performance [6]. Among various candidates, carbon nanotubes (CNTs) and graphene-based materials have emerged as the most prominent nanofillers due to their exceptional mechanical and physical properties. These materials have found widespread applications across diverse sectors, including aerospace, automotive, electronics and smart sensors, construction, and biomedical engineering. Fig. 1 illustrates the

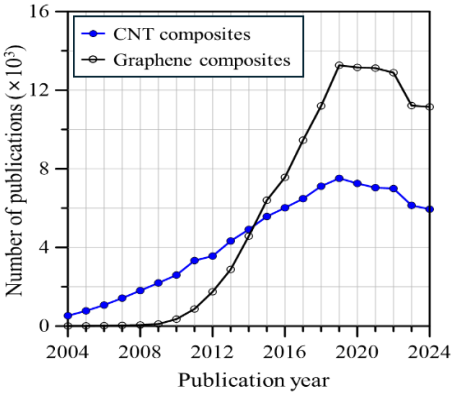

Fig. 1. Number of publications retrieved using the topic search terms "carbon nanotube composites" and "graphene composites" from 2004 to 2024 within the Clarivate Analytics database.

publication trends over the past two decades based on a topic search for "carbon nanotube composites" and "graphene composites" using the Clarivate Analytics database, confirming the continued research activity in this field.

The integration of nanomaterials into the wind turbine blades has been the focus of numerous studies. Ma and Zhang [7], for instance, evaluated the potential of CNT/polymer nanocomposites by examining both structural integrity and multifunctional capabilities, highlighting their superior mechanical strength, fatigue resistance, and thermal and electrical properties, while also pointing out challenges such as poor dispersion and high costs. Similarly, Buyuknalcari et al. [8] emphasized that the performance of CNT composites is strongly influenced by factors including nanotube diameter, alignment, interfacial interactions, and dispersion quality. Boncel et al. [9] presented a comprehensive review of the experimental and theoretical studies published to date, offering a systematic overview of the potential for CNT composites in wind blade applications. In contrast, despite the high potential of graphene-based materials as nanofillers, studies applying them to wind turbine blades have remained limited. Therefore, the authors of this study previously investigated the application of graphene platelets (GPLs) to a full scale wind blade model, analyzing key mechanical performances such as bending and vibration responses, deflection and stress concentration due to fatigue cracking, weight reduction, and cost effectiveness [10-13].

Despite the excellent mechanical performance of both CNTs and graphene-based fillers, their characteristics differ significantly in terms of mechanical properties, dispersion, fabrication, and cost-effectiveness, as demonstrated by Su et al. [6], who conducted a comprehensive analysis of multi-walled carbon nanotubes (MWCNTs)- and GPLs-reinforced nanocomposites. Punetha et al. [14] reviewed various covalent and non-covalent functionalization techniques applied to CNTs and graphene, and compared their effects on the mechanical, electrical, and thermal properties of the resulting composites, along with improvements in dispersion. They pointed out that, compared to CNTs, graphene presents greater challenges in dispersion or alignment using techniques such as mechanical stretching, electrical fields, magnetic fields, and spinning processes. Additional comparative studies have also been reported, including structural performance evaluations using finite element analysis (FEA) [15], and assessments of sensor applicability [16]. Given that material-level differences can significantly influence the structural behavior of large-scale composite systems such as wind turbine blades, the choice of nanofillers must be guided by a careful balance between structural reliability and economic viability, highlighting the importance of quantitative evaluation during the design process.

To address these issues, this study compares the structural performance of wind turbine blades reinforced with CNT- and graphene-based materials, focusing on bending and torsional stiffness, vibration behavior, and fatigue life. Furthermore, an economic analysis is performed to comprehensively assess the practical feasibility of CNT and graphene reinforcements. Section 2 details the material modeling techniques for the nanocomposites and the development of a full-scale finite element model of the wind turbine blade. Section 3 presents the results of the structural simulations and economic evaluation based on the developed model. Finally, Section 4 summarizes the main findings and significance of this study.

2. Finite element modeling

2.1 Material modeling

Nanocomposites reinforced with CNTs or graphene-based materials have attracted sustained interest in advanced materials engineering due to their exceptional combination of low weight and high strength. However, these materials are prone to aggregation within the composite matrix as a result of intermolecular interactions such as van der Waals forces and dipole–dipole interactions. This aggregation often leads to a deterioration of material properties, which remains a major unresolved issue highlighted in numerous studies. While the dispersion of CNTs can be improved to some extent through external forces, including mechanical stretching, electrical fields, and spinning processes, graphene-based reinforcements continue to pose significant challenges in terms of effective dispersion control [14]. In addition, the Halpin–Tsai model, which is widely used to estimate the properties of fiber-reinforced composites, has been reported to yield significantly reduced accuracy at higher weight fractions of reinforcement [17, 18]. To address these limitations, the present study restricts the weight fraction of nanofillers to a maximum of 0.3 wt%, based on the results shown in Fig. 2, in order to improve the accuracy of material modeling and minimize the influence of aggregation-related property degradation in nanocomposites.

It should also be noted that the use of single-walled carbon nanotubes (SWCNTs) and monolayer graphene sheets in industrial applications remains limited due to their substantially high production costs. In this study, therefore, the analysis focused on more cost-effective alternatives: MWCNTs and GPLs.

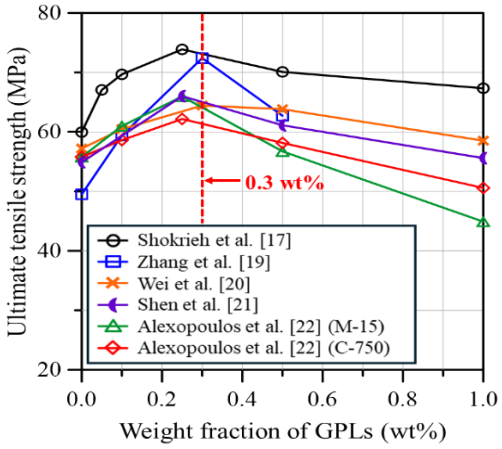

Fig. 2. Variation in ultimate tensile strength of GPL-reinforced nanocomposites due to GPL content and aggregation.

The Poisson's ratio v and the density ρ of the resulting nanocomposites, namely carbon nanotube reinforced composites (CNTRCs) and graphene platelet reinforced composites (GPLRCs), were calculated using the rule of mixtures given by

$$M_{eff} = M_{nano} V_{nano} + M_m V_m \tag{1}$$

Here, M and V denote the material property and volume fraction, while the subscripts *eff*, *nano*, and *m* refer to the effective property of the nanocomposite, the nanofiller, and the matrix, respectively.

In contrast, the elastic modulus E was estimated with higher accuracy using the Halpin–Tsai model [23,24], which considers the size and shape of the nanofillers, which is given by

$$E_{eff} = \frac{3}{8}\cdot\frac{1+\alpha(A-1)V_I/(A+\alpha)}{1-(A-1)V_I/(A+\alpha)}\times E_m + \frac{5}{8}\cdot\frac{1+2(A-1)V_I/(A+2)}{1-(A-1)V_I(A+2)}\times E_m \tag{2}$$

with $\alpha = 2\ell_{CNT}/d_{CNT}$, $A = 4t_{CNT}E_{CNT}/(d_{CNT}E_m)$, $V_I = V_{CNT}$ for CNTRC. Here, ℓ_{CNT}, d_{CNT}, and t_{CNT} denote the length, diameter, and wall thickness of the CNT, respectively. The values used in this study are $\ell_{CNT} = 20\mu m$, $d_{CNT} = 20nm$, $t_{CNT} = 1.5nm$. For GPLRC, $\alpha = (W+L)/t$, $A = E_{GPL}/E_m, V_I = V_{GPL}$. Here, L, W, and t represent the length, width, and thickness of the GPLs, respectively. In this study, the values were set to $L = 2.5\mu m$, $W = 1.5\mu m$, and $t = 1.5nm$ [24].

This study assumed that the MWCNTs and GPLs were uniformly dispersed and exhibited isotropic behavior within the matrix. Table 1 presents the material properties of the matrix and nanofillers used in the study, along with the calculated properties of the nanocomposites based on Eqs. (1) and (2).

As highlighted by Kim and Cho [25], a full replacement of glass fiber reinforced composites in wind turbine blades with nanocomposites such as CNTRCs or GPLRCs may lead to a significant reduction in fatigue life due to the relatively poor fatigue performance of nanocomposite materials. To address this issue with a more practical and realistic approach, this study considers a limited application in which only the matrix of the conventional glass fiber composite is substituted with a nanocomposite. Accordingly, it should be clearly noted that the weight fractions of nanofillers specified in this study are defined with respect to the matrix material, not the entire glass fiber reinforced composite (GFRP).

Table 1. Material properties of Epoxy (matrix), nanofillers, and nanocomposites.

Material	E (GPa)	v_{12}	ρ (kg/m^3)
Epoxy	3	0.340	1200
MWCNT	450	0.305	624
GPL	1010	0.186	1060
0.1 wt% MWCNT	3.10	0.340	1199
0.2 wt% MWCNT	3.21	0.340	1198
0.3 wt% MWCNT	3.31	0.340	1197
0.1 wt% GPL	3.39	0.340	1200
0.2 wt% GPL	3.77	0.340	1200
0.3 wt% GPL	4.16	0.339	1200

Table 2. Material properties of SNL(Triax): experimentally characterized by Resor [26] and theoretically evaluated in the present study.

SNL (Triax)	E_{11} (GPa)	E_{22} (GPa)	G_{12} (GPa)	v_{12}	ρ (kg/m^3)
Neat GFRP [26]	27.70	13.65	7.20	0.39	1850
Neat GFR (Present)	27.74	12.48	8.23	0.38	1850
0.1 wt% MWCNT	27.94	12.81	8.31	0.38	1849
0.2 wt% MWCNT	28.14	13.15	8.40	0.38	1849
0.3 wt% MWCNT	28.33	13.47	8.48	0.38	1849
0.1 wt% GPL	28.47	13.72	8.54	0.38	1850
0.2 wt% GPL	29.18	14.90	8.84	0.38	1850
0.3 wt% GPL	29.86	16.04	9.13	0.38	1850

The wind turbine blade model used in this study is based on the SNL (Triax) composite, a material fabricated by combining unidirectional and bidirectional glass fiber laminates—specifically, E-LT-5500 (UD) and Saertex (DB). To accurately determine the material properties of SNL (Triax), the properties of E-LT-5500 (UD) and Saertex (DB) were theoretically derived. The Halpin–Tsai model was employed for E-LT-5500 (UD), while classical laminate theory was applied to Saertex (DB). The reliability of the derived theoretical values was validated by comparing them with experimental data reported by Resor [26]. Tables A1 and A2 in Appendix present a comparison between the theoretical and experimental properties of E-LT-5500 (UD) and Saertex (DB), while Table 2 summarizes the resulting properties of the combined SNL (Triax) composite, which is hereafter referred to as GFRP, along with those of the nanocomposite-reinforced GFRP.

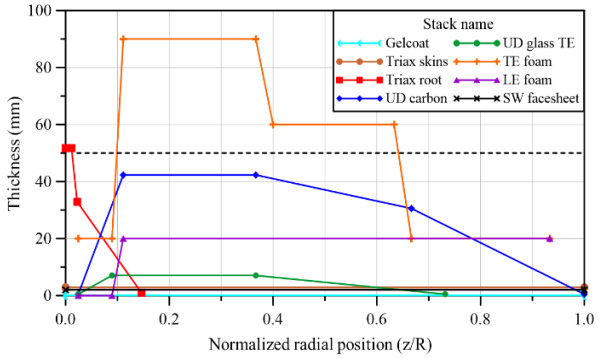

Fig. 3. Developed finite element model and thickness distributions of each composite material along the blade span (*z*: radial position, *R*: blade span) [25].

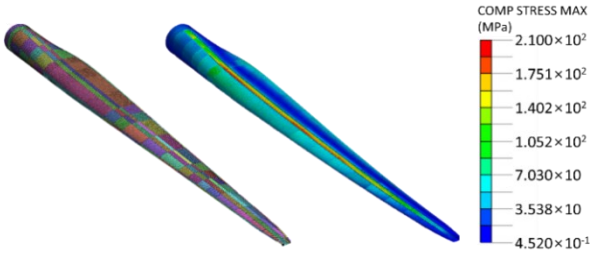

Fig. 4. Developed 5MW SNL 61.5 m wind turbine blade model: finite element model (left) and stress distribution under the rated wind speed (right).

2.2 Blade modeling

Wind turbine blades are typically composed of laminated composites in which various materials are functionally distributed to meet structural requirements. To ensure high accuracy in computational analysis, it is essential to precisely model not only the blade geometry but also the detailed configuration of the composite layups. In this study, a 5MW-class wind turbine blade was selected as the reference model for finite element analysis. The geometry and material modeling of the blade was developed based on the design data of the SNL 61.5 m blade model reported by Resor [26]. The blade geometry accounts for spanwise variations in airfoil profiles, chord length, twist angle, and aerodynamic center. The composite layups were modeled to vary according to the spanwise location and across seven key structural sections: the leading edge (LE), LE panel, spar cap, trailing edge (TE), TE reinforcement, TE panel, and shear web. Fig. 3 illustrates the variation in thickness of each composite material along the blade span. Additional details on the blade model can be found in the report by Resor [26].

In aerodynamic load analysis of wind turbine blades, computational fluid dynamics (CFD) and blade element momentum theory (BEMT) are commonly employed. In this study, aerodynamic loads were computed using BEMT, which offers a balance between computational efficiency and accuracy. The detailed methodology for aerodynamic load calculations based on BEMT can be found in the authors' previous publications [10,12]. Fig. 4 presents the stress distribution at the rated wind speed of 11.4 *m/s*, as obtained from the finite element model developed in this study.

Table 3. Material mass distribution in the SNL 61.5 m wind turbine blade.

Model	Mass (kg)						
	Gelcoat	E-LT-5500 (UD)	Saertex (DB)	SNL (Triax)	Foam	Carbon (UD)	Total
Present	29	338	921	8726	4160	2655	16829
Chen et al. [30]	29	376	916	8784	3953	2638	16696

Table 4. Natural frequency of the SNL 61.5 m wind turbine blade.

Model	Natural frequency (Hz)					
	1st Flap-wise	1st Edge-wise	2nd Flap-wise	2nd Edge-wise	3rd Flap-wise	1st Tors-ion
Present	0.842	0.993	2.727	3.592	5.726	6.728
Resor [26]	0.870	1.060	2.680	3.910	5.570	6.450
Shakya et al. [31]	0.900	-	2.850	-	6.410	6.650
Johnson & Hsu [32]	0.919	1.055	2.811	3.887	5.690	6.715
Thapa & Missoum [33]	0.840	0.969	2.410	-	-	-

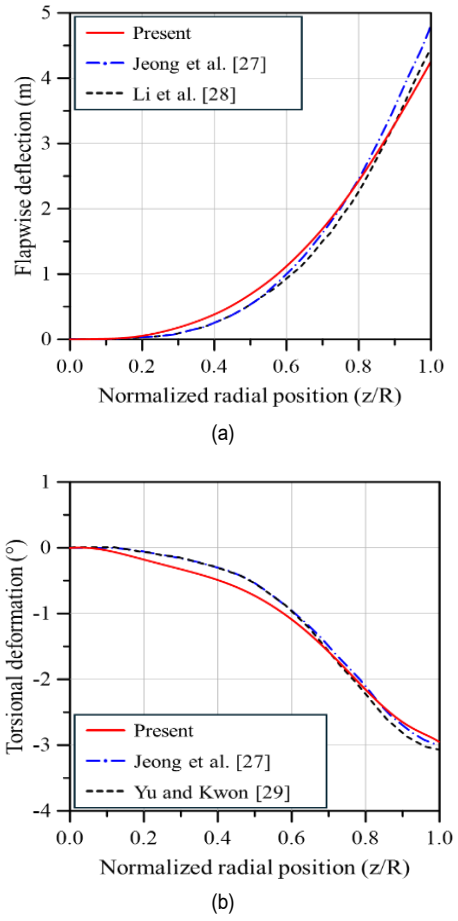

Fig. 5. Deflections of the SNL 61.5 m wind turbine blade (z: radial position, R: blade span): (a) flapwise, (b) torsional.

To ensure the validity of the various analyses and results presented in Section 3, it is essential to verify the reliability of the wind turbine blade model developed in this study. For numerical simulation, the commercial finite element analysis software midas-NFX was used. The analysis model was created using four-node quad elements, with an element size of 0.08 meters by 0.08 meters, consistent with the mesh size reported in Resor [26]. To accurately capture the laminated composite structure of the blade and its load transfer behavior, 'composite shell properties' within midas-NFX were assigned to the elements. Tables 3 and 4 compare the mass and natural frequencies of the present model with those from previous studies, while Fig. 5 presents a comparison of deflection and torsional deformation behavior. The results indicate a good agreement in mechanical characteristics between the present and reference models, confirming the reliability of the simulation results of this study.

3. Numerical results

In the design of engineering structures, a thorough evaluation of both mechanical performance and cost-effectiveness is essential to ensure structural safety and long-term sustainability. This becomes particularly important when advanced materials such as nanocomposites are introduced, as uncertainties in their behavior may lead to unexpected outcomes. In this context, the present study aims to assess the structural performance and cost-effectiveness of wind turbine blades reinforced with either MWCNTs or GPLs, and to evaluate the applicability of these nanocomposites in wind blades. This section presents a systematic analysis in which the MWCNT- and GPL-reinforced glass fiber composites, developed using the Halpin-Tsai model and classical laminate theory as described in Section 2, are applied to the validated wind turbine blade model. The resulting bending and torsional behavior, vibration characteristics, fatigue performance, and cost analysis are comprehensively examined.

3.1 Static bending and torsional deformation

As shown in Fig. 6, the deflection behavior of wind turbine blades is generally categorized into flapwise and edgewise directions. Among these, flapwise deflection tends to be greater than edgewise deflection due to the influence of aerodynamic loads. In evaluating the global structural response of engineering systems, it is important to consider not only bending deformation but also torsional deformation. For wind turbine blades in particular, torsional behavior about the spanwise axis is a critical factor in structural reliability. Table 5 presents the relative reductions in maximum flapwise and edgewise deflections, as well as torsional deformation, with respect to the weight fraction of nanofillers when MWCNT- and GPL-reinforced glass fiber composites are applied to the blade. The results indicate that increasing the weight fraction of nanofillers leads to an overall reduction in deformation, which is attributed to the improved stiffness of the glass fiber composites. Among the different deformation modes, torsional deformation showed the greatest reduction, followed by edgewise and then flapwise deflection. Notably, even at a low reinforcement level of 0.3 wt%, the maximum torsional deformation was reduced by approximately 11 percent with MWCNTs and 16 percent with GPLs. These findings suggest that reinforcing glass fiber composites with nanomaterials can provide meaningful structural enhancement without a significant increase in blade weight, and that GPLs may offer greater reinforcement effectiveness than MWCNTs. While presenting higher nanofiller weight fractions could make the observed trend more evident, contents beyond 0.3 wt% were intentionally excluded to prevent modeling uncertainties, as outlined in Section 2.1.

Table 5. Relative reductions (%) in maximum flapwise, edgewise, and torsional deformations with respect to Neat GFRP.

Deflection mode	MWCNTs			GPLs		
	0.1 wt%	0.2 wt%	0.3 wt%	0.1 wt%	0.2 wt%	0.3 wt%
Flapwise	-0.22	-0.37	-0.53	-0.65	-1.12	-1.66
Edgewise	-0.85	-1.71	-2.58	-3.33	-5.53	-8.89
Torsional	-9.66	-10.49	-11.32	-11.34	-13.72	-15.99

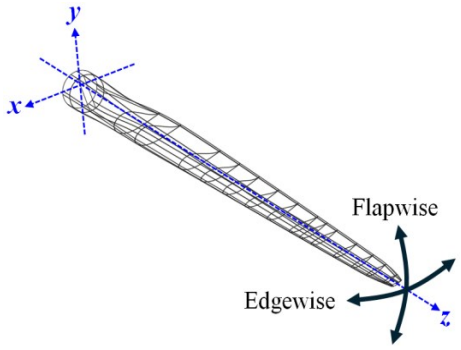

Fig. 6. Deflection directions of a wind turbine blade.

3.2 Free vibration

Vibration characteristics are considered a critical factor in evaluating the safety of rotating structures., In the case of wind turbine blades, the potential for resonance must be carefully examined during the design and verification stages. In this study, the natural frequencies of wind turbine blades reinforced with MWCNTs and GPLs were analyzed, and the results are summarized in Table 6. The analysis showed that, in all reinforced cases, the natural frequencies increased compared to those of the neat GFRP blade. This trend was more pronounced when GPLs were used as reinforcement, indicating a greater impact on stiffness than MWCNTs.

When evaluating the vibration characteristics of rotating structures such as wind turbine blades, Campbell diagrams are widely used to visualize the interaction between natural frequencies and estimated excitation frequencies, thereby enabling the

Table 6. Natural frequencies of wind turbine blades with and without nanofillers.

Mode	Natural frequency (*Hz*)						
	Neat GFRP	MWCNTs			GPLs		
		0.1 wt%	0.2 wt%	0.3 wt%	0.1 wt%	0.2 wt%	0.3 wt%
1	0.8415	0.8435	0.8449	0.8463	0.8475	0.8520	0.8563
2	0.9930	0.9944	0.9966	0.9988	1.0009	1.0087	1.0166
3	2.7269	2.7406	2.7434	2.7462	2.7483	2.7573	2.7662
4	3.5918	3.5905	3.6022	3.6141	3.6240	3.6637	3.7028
5	5.7255	5.7817	5.7918	5.8026	5.8079	5.8400	5.8699
6	6.7280	7.0442	7.0785	7.1158	7.1214	7.2296	7.3344

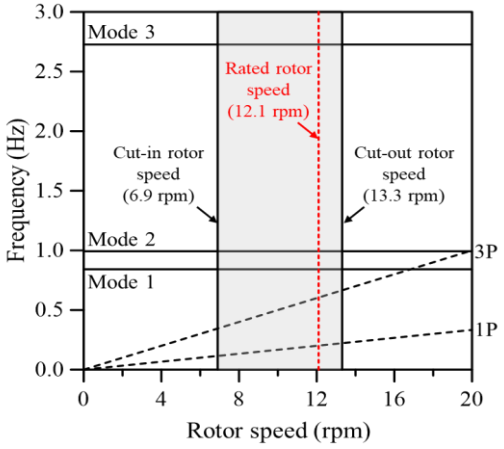

Fig. 7. Campbell diagram of the wind turbine blade composed of neat GFRP.

assessment of potential resonance conditions. Fig. 7 presents the Campbell diagram for a wind turbine blade made of neat GFRP. In this diagram, 1P refers to the rotor's rotational frequency, while 3P corresponds to the blade shadowing frequency, which occurs as the blade passes in front of the tower. These are critical harmonic excitations that must be considered in blade design. As shown in Fig. 7, the natural frequencies of the neat GFRP blade do not intersect with either 1P or 3P within the typical operating speed range of the rotor, indicating a low likelihood of resonance. Furthermore, when nanofillers are introduced, the first and second mode natural frequencies increase (see Table 6), which widens the separation from harmonic excitations and enhances resonance safety. In particular, the blade reinforced with GPLs exhibits higher natural frequencies than the one reinforced with MWCNTs, suggesting that GPLs offer better structural safety against potential resonance.

3.3 Fatigue life estimation

Wind turbine blades are continuously subjected to cyclic wind loads and unpredictable environmental conditions throughout their service life. These factors can adversely affect the long-term structural integrity of the blade. Among them, fatigue caused by repeated loading is one of the primary mechanisms

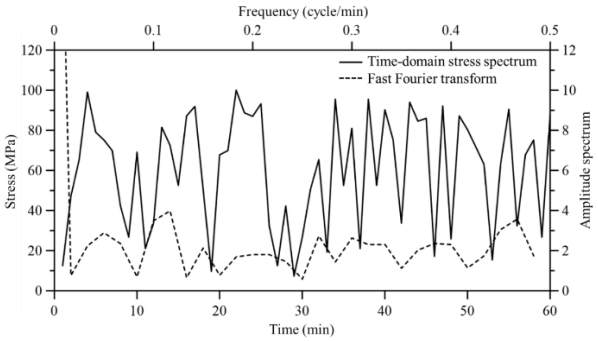

Fig. 8. Illustration of stress time history and its corresponding transformation into the frequency domain.

that compromise structural health, as micro-defects can accumulate over time, develop into cracks, and eventually lead to failure. Therefore, quantitative evaluation of fatigue life, alongside yielding and buckling, is a critical design consideration in the structural analysis of wind turbine blades. Based on this context, this section presents a comparative analysis of the fatigue life of wind turbine blades reinforced with MWCNTs and GPLs, respectively.

The ideal approach for evaluating the fatigue life of wind turbine blades is to apply a long-term fatigue load spectrum that reflects the entire design life of the structure. However, directly acquiring long-duration time histories of wind speed and using it for experimental or numerical fatigue life assessment is often impractical due to the significant cost and time required. Therefore, in engineering practice, alternative methods that rely on short-term data combined with probabilistic modeling are commonly adopted to estimate long-term structural responses. In this study, to simulate realistic wind conditions, short-term wind speed data over a 60-minute period was generated based on long-term observations at European offshore wind farms, which follow a Weibull distribution with shape parameter α = 2.0 and scale parameter β = 15.0 as given by Zhang et al. [34]:

$$f(x)=\frac{\alpha}{\beta}\left(\frac{x}{\beta}\right)^{\alpha-1}\exp\left[-\left(\frac{x}{\beta}\right)^{\alpha}\right] \tag{3}$$

Wind turbine blades operate under highly irregular and variable environmental conditions, which result in complex load cycles that include various frequencies. To evaluate the accumulated fatigue damage in the blade, these complex stress cycles must be decomposed into their frequency components to define the corresponding stress amplitudes. In this study, aerodynamic loads corresponding to each wind speed were calculated using BEMT, and these loads were applied to a finite element model to extract time-domain stress data. A fast Fourier transform (FFT) was then used to convert the time-domain stress responses into the frequency domain. Fig. 8 illustrates an example of the stress response obtained in the time domain and the corresponding fatigue load spectrum after frequency-domain transformation.

Table 7. Material properties of the neat GFRP and GFRP composites reinforced with MWCNTs and GPLs for fatigue life assessment.

Material properties	Neat GFRP	MWCNTs (0.2 wt%)	GPLs (0.2 wt%)
σ_u (*MPa*)	700	820	926
b	10.00	10.46	10.36

The S–N curves commonly used for fatigue life evaluation are typically derived under zero mean stress conditions. As a result, they do not adequately represent the complex stress environments experienced by real structures, where alternating and mean stresses coexist. To address this limitation, the concept of equivalent stress was introduced to account for the effect of mean stress. In this study, equivalent stress was calculated using the Goodman diagram, as follows

$$\sigma_{eqa} = \frac{\sigma_a\left(\sigma_{eqm} - \sigma_u\right)}{\sigma_m - \sigma_u} \tag{4}$$

where, σ_{eqa} is the equivalent stress corresponding to the equivalent mean stress σ_{eqm}, which is 0 in this study, σ_a is the amplitude stress, and σ_m is the mean stress, σ_u is the ultimate stress of the material . By applying the resulting equivalent stress to the material's S–N curve, the number of cycles to fatigue failure *N* can be estimated according to

$$N = \left(\frac{\sigma_{eqa}}{\sigma_u}\right)^{-b} \tag{5}$$

where, *N* is the number of cycles to failure, σ_u is the ultimate strength of material, σ_{eqa} is the equivalent stress, and b is inverse of the slope of the S-N curve.

Table 7 summarizes the material properties of the glass fiber composites used in this study for calculating the number of cycles to fatigue failure *N* based on Eq. (5). The table includes the properties of neat GFRP as well as those of the composites reinforced with 0.2 wt% of MWCNTs and GPLs. The properties of neat GFRP were adopted from Resor [26], while the values for the MWCNT- and GPL-reinforced composites were estimated by incorporating the stress increase ratio corresponding to the number of cycles to failure, as reported in the fatigue test results of Yavari [35]. While nanocomposites showed the best performance at 0.3 wt%, material properties for fatigue life assessment (e.g., S-N curves) are limitedly reported in the literature. To obtain reliable outcomes, 0.2 wt% of nanofillers was selected in this study, as the required material data is documented in the literature [35]. Fig. 9 presents the S–N curves developed using these material properties.

Subsequently, the accumulated fatigue damage can be evaluated based on the number of fatigue cycles and the number of corresponding cycles from each stress amplitude to failure. In this study, the accumulated fatigue damage was calculated using Miner's rule, which is defined by

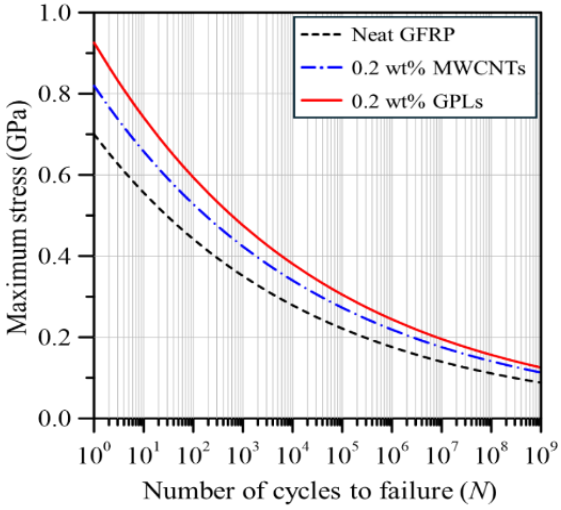

Fig. 9. S–N curves of neat GFRP and GFRP composites reinforced with MWCNTs and GPLs.

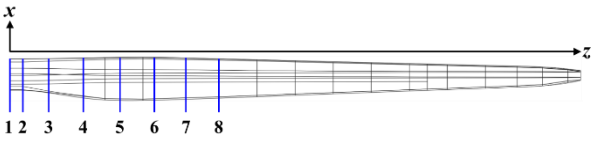

Location	1	2	3	4	5	6	7	8
Span location z (m)	0	1.3667	4.1	6.8333	10.25	14.35	18.45	22.55

Fig. 10. Spanwise location for fatigue life analysis.

$$D = \sum_{i=1}^{n} \frac{n_i}{N_i} \tag{6}$$

where *D* is the cumulative fatigue damage, n_i and N_i are the numbers of the load cycles and cycles to failure, respectively. The fatigue life of the blade was then determined using the accumulated damage, as given by

$$\text{Fatigue life (years)} = \frac{1}{\sum D \times 24 \times 365} \tag{7}$$

The fatigue life was evaluated by dividing the blade region into twenty sub-regions, as shown in Fig. 10, and the fatigue lives of critical eight sub-regions from the blade root are presented in this paper.

Fig. 11 and Table 8 present the predicted fatigue life of wind turbine blades along the spanwise direction, comparing blades made of neat GFRP with those reinforced with MWCNTs and GPLs. Where, "Location" refers to the spanwise position along the blade, as shown in Fig. 10. The results indicate that nanomaterial reinforcement leads to a substantial improvement in fatigue life relative to the neat GFRP case. Between the two reinforced cases, the blade incorporating GPLs demonstrated superior fatigue resistance. Notably, at Location 5—where the

Table 8. Fatigue life of wind turbine blades made of neat GFRP and GFRP composites reinforced with MWCNTs and GPLs.

Location	Fatigue life (years)		
	Neat GFRP	0.2 wt% MWCNTs	0.2 wt% GPLs
1	1.86×10^{8}	3.22×10^{9}	8.27×10^{9}
2	9.05×10^{7}	1.46×10^{9}	3.81×10^{9}
3	4.80×10^{7}	8.42×10^{8}	1.96×10^{9}
4	2.00×10^{5}	2.76×10^{6}	6.71×10^{6}
5	6.81×10^{1}	6.15×10^{2}	1.78×10^{3}
6	1.06×10^{3}	1.01×10^{4}	2.86×10^{4}
7	2.16×10^{3}	2.09×10^{4}	5.96×10^{4}
8	9.71×10^{3}	9.56×10^{4}	2.64×10^{5}

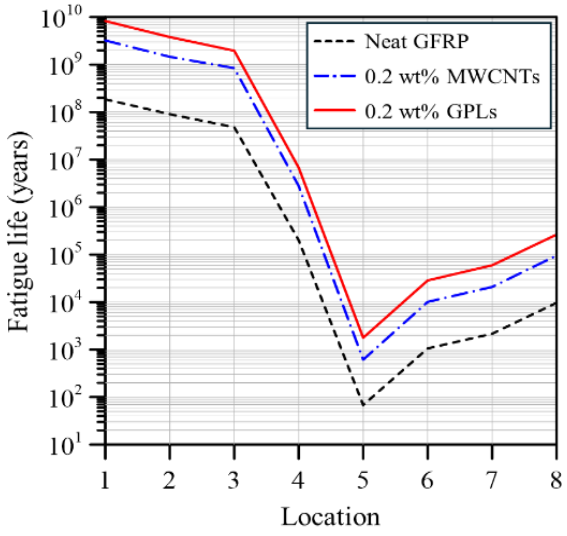

Fig. 11. Fatigue life of wind turbine blades made of neat GFRP and GFRP composites reinforced with MWCNTs and GPLs.

shortest fatigue life was predicted—the neat GFRP blade had an estimated life of approximately 68 years, while the blades reinforced with MWCNTs and GPLs showed substantial increases, reaching around 615 years and 1,780 years, respectively. These results suggest that even a small addition of 0.2 wt% nanofillers to the matrix of glass fiber composites can lead to remarkable improvements in fatigue durability. Moreover, the enhancement appears to be more pronounced with GPL reinforcement than with MWCNTs.

3.4 Cost-benefit analysis

This section analyzes the economic feasibility of applying the two types of nanofillers to wind turbine blades, with a focus on comparing the total material cost required for blade fabrication. The unit prices of the primary materials used in this study are summarized in Table 9. Based on these values, the total material cost for a single blade is estimated to be approximately 138,288 USD. Given that 0.3 wt% of neat GFRP matrix corresponds to about 12 kilograms, the additional material cost

Table 9. Material costs of wind turbine blades (Bortolotti et al. [36], Su et al. [6]).

Material	Cost (USD/kg)	Mass (kg)		
		Neat GFRP	0.3 wt% MWCNTs	0.3 wt% GPLs
Gelcoat	7.23	29	29	29
E-LT-5500 (UD)	1.87	338	338	338
Saertex (DB)	3.00	921	921	921
SNL (Triax)	2.86	8726	8726	8726
Foam	7.23	4160	4160	4160
Carbon (UD)	30.00	2655	2655	2655
MWCNT	30.00	-	12	-
GPL	20.00	-	-	12
Total weight (kg)		16829	16841	16841
Total cost (USD)		138,288	138,648	138,528

incurred by incorporating MWCNTs and GPLs is approximately 360 USD and 240 USD, respectively. These values account for less than 0.3 percent of the total material cost. Considering the associated improvements in structural stiffness and fatigue life, the use of these nanofillers appears to be economically feasible. However, since this analysis does not account for production costs, labor, or other associated expenses, a more comprehensive economic analysis would be required for practical implementation.

4. Conclusion

This study investigated the structural performance, dynamic response, fatigue resistance, and cost-effectiveness of wind turbine blades enhanced with CNT and graphene-based nanofillers, using the 61.5-meter SNL blade as a 5 MW-class reference model for the simulations. The developed numerical model was validated by comparing key results such as deflection, torsion, material mass, and natural frequencies with values reported in the literature. As nanofillers, MWCNTs and GPLs were selected based on their cost-effectiveness and practical applicability. These nanofillers were incorporated into the matrix of the SNL(Triax) composite, which was used as the primary material for the blade model.

Structural performance and fatigue life were evaluated for wind turbine blades incorporating small amounts (0.1 to 0.3 wt%) of MWCNT- and GPL-reinforced nanocomposites. Compared to neat GFRP, both nanofillers improved bending, torsion, and vibration characteristics. Notably, GPL reinforcement yielded more pronounced enhancements in structural performance compared to MWCNTs. Fatigue life analysis was then carried out for blades reinforced with 0.2 wt% of each nanofiller. In the midspan region, where the most critical loading conditions are observed, the fatigue life increased substantially, rising from about 68 years for the neat GFRP blade to approximately 615 years with MWCNT reinforcement and 1,780 years with GPL reinforcement. From a cost perspective, the incorporation of

nanofillers increased the overall material cost of the blade by less than 0.3%, indicating that such reinforcement can be implemented without compromising economic feasibility. Nanocomposites reinforced with MWCNTs and GPLs appear to be promising solutions for improving both the structural performance and service life of wind turbine blades. Between the two, GPL reinforcement demonstrates greater potential in terms of both structural efficiency and cost-effectiveness.

While the present study demonstrates the advantages of CNT and graphene-based nanofillers for wind turbine blade applications, further studies are needed to refine their optimal content and distribution within the composite. Follow-up investigations are underway to address these aspects in more depth.

Acknowledgments

This work was supported by 2025 Hongik University Research Fund. This work was supported by the National Research Foundation of Korea (NRF) grant funded by the Korea government (MSIT) (2020R1A2C1100924, RS-2023-00240618).

References

[1] N. M. Chikhradze, F. D. S. Marquis and G. S. Abashidze, Hybrid fiber and nanopowder reinforced composites for wind turbine blades, *Journal of Materials Research and Technology*, 4 (1) (2015) 60-67.

[2] A. N. Mengal, S. Karuppanan and A. A. Wahab, Basalt carbon hybrid composite for wind turbine rotor blades: A short review, *Advanced Materials Research*, 970 (2014) 67-73.

[3] J. Paquette, J. van Dam and S. Hughes, Structural testing of 9m carbon fiber wind turbine research blades, *45th AIAA Aerospace Sciences Meeting and Exhibit*, AIAA, Reno, Nevada, USA (2007).

[4] J. W. Holmes, P. Brøndsted, B. F. Sørensen, Z. Jiang, Z. Sun and X. Chen, Development of a bamboo-based composite as a sustainable green material for wind turbine blades, *Wind Engineering*, 33 (2) (2009) 197-210.

[5] J. Shen-xue, Z. Qi-sheng and J. Shu-hai, On structure, production, and market of bamboo-based panels in China, *Journal of Forestry Research*, 13 (2) (2002) 151-156.

[6] X. Su, R. Wang, X. Li, S. Araby, H. C. Kuan, M. Naeem and J. Ma, A comparative study of polymer nanocomposites containing multi-walled carbon nanotubes and graphene nanoplatelets, *Nano Materials Science*, 4 (3) (2022) 185-204.

[7] P. C. Ma and Y. Zhang, Perspectives of carbon nanotubes/polymer nanocomposites for wind blade materials, *Renewable and Sustainable Energy Reviews*, 30 (2014) 651-660.

[8] F. N. Buyuknalcaci, Y. Polat, T. A. Negawo, E. Döner, M. S. Alam, T. Hamouda and A. Kilic, Carbon nanotube-based nanocomposites for wind turbine applications, in *Polymer-based Nanocomposites for Energy and Environmental Applications*, M. Jawaid and M. M. Khan (eds), Woodhead Publishing, UK (2018) 635-661.

[9] S. Boncel, A. Kolanowska, A. W. Kuziel and I. Krzyżewska, Carbon nanotube wind turbine blades: How far are we today from laboratory tests to industrial implementation?, *ACS Applied Nano Materials*, 1 (12) (2018) 6542-6555.

[10] H. J. Kim and J. R. Cho, Effects of graphene reinforcement on static bending, free vibration, and torsion of wind turbine blades, *Materials*, 17 (13) (2024) 3332.

[11] H. J. Kim and J. R. Cho, Exploratory study on the application of graphene platelet-reinforced composite to wind turbine blade, *Polymers*, 16 (14) (2024) 2002.

[12] H. J. Kim and J. R. Cho, In-depth study on the application of a graphene platelet-reinforced composite to wind turbine blades, *Materials*, 17 (16) (2024) 3907.

[13] H. J. Kim and J. R. Cho, Numerical study on the static bending response of cracked wind turbine blades reinforced with graphene platelets, *Nanomaterials*, 14 (24) (2024) 2020.

[14] V. D. Punetha, S. Rana, H. J. Yoo, A. Chaurasia, J. T. McLeskey, M. S. Ramasamy, N. G. Sahoo and J. W. Cho, Functionalization of carbon nanomaterials for advanced polymer nanocomposites: A comparison study between CNT and graphene, *Progress in Polymer Science*, 67 (2017) 1-47.

[15] N. Gariya and A. Shaikh, Comparative analysis between graphene and carbon nanotube reinforced epoxy composite, *Materials Today: Proceedings*, in press (2023).

[16] X. Wang, E. G. Lim, K. Hoettges and P. Song, A review of carbon nanotubes, graphene and nanodiamond based strain sensor in harsh environments, *C*, 9 (4) (2023) 108.

[17] M. Shokrieh, M. Esmkhani, H. R. Shahverdi and F. Vahedi, Effect of graphene nanosheets (GNS) and graphite nanoplatelets (GNP) on the mechanical properties of epoxy nanocomposites, *Science of Advanced Materials*, 5 (2012) 260-266.

[18] Y. Zare and K. Y. Rhee, The mechanical behavior of CNT reinforced nanocomposites assuming imperfect interfacial bonding between matrix and nanoparticles and percolation of interphase regions, *Composites Science and Technology*, 144 (2017) 18-25.

[19] Y. Zhang, Y. Wang, J. Yu, L. Chen, J. Zhu and Z. Hu, Tuning the interface of graphene platelets/epoxy composites by the covalent grafting of polybenzimidazole, *Polymer*, 55 (19) (2014) 4990-5000.

[20] J. Wei, R. Atif, T. Vo and F. Inam, Graphene nanoplatelets in epoxy system: dispersion, reaggregation, and mechanical properties of nanocomposites, *Journal of Nanomaterials*, 2015 (1) (2015) 561742.

[21] M.-Y. Shen, T.-Y. Chang, T.-H. Hsieh, Y.-L. Li, C. L. Chiang, H. Yang and M.-C. Yip, Mechanical properties and tensile fatigue of graphene nanoplatelets reinforced polymer nanocomposites, *Journal of Nanomaterials*, 2013 (2013) 565401.

[22] N. D. Alexopoulos, Z. Paragkamian, P. Poulin and S. K. Kourkoulis, Fracture related mechanical properties of low and high graphene reinforcement of epoxy nanocomposites, *Composites Science and Technology*, 150 (2017) 194-204.

[23] J. C. Halpin and J. L. Kardos, The Halpin-Tsai equations: A review, *Polymer Engineering & Science*, 16 (5) (1976) 344-352.

[24] M. A. Rafiee, J. Rafiee, Z. Wang, H. Song, Z. Z. Yu and N.

Koratkar, Enhanced mechanical properties of nanocomposites at low graphene content, *ACS Nano*, 3 (12) (2009) 3884-3890.
[25] H. J. Kim and J. R. Cho, Numerical analysis of fatigue life of wind turbine blades reinforced with graphene platelets, *Applied Sciences*, 15 (4) (2025) 1866.
[26] B. R. Resor, Definition of a 5 MW/61.5 m wind turbine blade reference model, *Technical Report* SAND2013-2569; 463454, Sandia National Laboratories, Albuquerque, NM, USA (2013).
[27] M. S. Jeong, M. C. Cha, S. W. Kim, I. Lee and T. Kim, Effects of torsional degree of freedom, geometric nonlinearity, and gravity on aeroelastic behavior of large-scale horizontal axis wind turbine blades under varying wind speed conditions, *Journal of Renewable and Sustainable Energy*, 6 (2) (2014) 023126.
[28] Z. Li, B. Wen, X. Dong, Z. Peng, Y. Qu and W. Zhang, Aerodynamic and aeroelastic characteristics of flexible wind turbine blades under periodic unsteady inflows, *Journal of Wind Engineering and Industrial Aerodynamics*, 197 (2020) 104057.
[29] D. O. Yu and O. J. Kwon, A coupled CFD-CSD method for predicting HAWT rotor blade performance, *51st AIAA Aerospace Sciences Meeting including the New Horizons Forum and Aerospace Exposition*, AIAA, Grapevine, Texas, USA (2013).
[30] Z. J. Chen, K. A. Stol and B. R. Mace, Wind turbine blade optimisation with individual pitch and trailing edge flap control, *Renewable Energy*, 103 (2017) 750-765.
[31] P. Shakya, M. R. Sunny and D. K. Maiti, A parametric study of flutter behavior of a composite wind turbine blade with bend-twist coupling, *Composite Structures*, 207 (2019) 764-775.
[32] E. L. Johnson and M. C. Hsu, Isogeometric analysis of ice accretion on wind turbine blades, *Computational Mechanics*, 66 (2) (2020) 311-322.
[33] M. Thapa and S. Missoum, Uncertainty quantification and global sensitivity analysis of composite wind turbine blades, *Reliability Engineering & System Safety*, 222 (2022) 108354.
[34] C. Zhang, H. P. Chen and T. L. Huang, Fatigue damage assessment of wind turbine composite blades using corrected blade element momentum theory, *Measurement*, 129 (2018) 102-111.
[35] F. Yavari, M. A. Rafiee, J. Rafiee, Z. Z. Yu and N. Koratkar, Dramatic increase in fatigue life in hierarchical graphene composites, *ACS Applied Materials & Interfaces*, 2 (10) (2010) 2738-2743.
[36] P. Bortolotti, D. Berry, R. Murray, E. Gaertner, D. Jenne, R. Damiani, G. Barter and K. Dykes, A detailed wind turbine blade cost model, *Technical Report* NREL/TP-5000-73585, National Renewable Energy Laboratory (NREL), USA (2019).

Appendix

A. Material properties of E-LT-5500 (UD) and Saertex (DB)

Table A1. Material properties of E-LT-5500 (UD): experimentally characterized by Resor [26] and theoretically evaluated in the present study.

E-LT5500 (UD)	V_f	E_{11} (*GPa*)	E_{22} (*GPa*)	G_{12} (*GPa*)	v_{12}	ρ (kg/m^3)
Resor [26]	0.54	41.80	14.00	2.63	0.28	1920
Present	0.54	41.83	11.31	3.35	0.28	1800

* V_f: volume fraction of glass fibers, G: shear modulus.

Table A2. Material properties of Saertex(DB): experimentally characterized by Resor [26] and theoretically evaluated in the present study.

Saertex (DB)	V_f	E_{11} (*GPa*)	E_{22} (*GPa*)	G_{12} (*GPa*)	v_{12}	P (kg/m^3)
Resor [26]	0.44	13.60	13.30	11.80	0.49	1780
Present	0.63	13.58	13.58	13.07	0.49	1900

* V_f: volume fraction of glass fibers.

Hyeong Jin Kim received his B.S. degree from Hongik University in 2020 and his M.S. degree from Pusan National University in 2022. He currently is a PhD student in the Department of Mechanical Engineering at University College London. His research focuses on the safety engineering of ships and offshore structures, encompassing digital healthcare engineering (DHE) systems, structural design optimization, nonlinear structural mechanics, and nonlinear finite element analysis.

Jin-Rae Cho received his B.S. degree in Aeronautical Engineering from Seoul National University in 1983. He then received his M.S. and Ph.D. degrees from The University of Texas at Austin in 1993 and 1995, respectively. He is currently a Professor in Department of Naval Architecture and Ocean Engineering at Hongik University. His major research field is the computational mechanics in solid/structural mechanics, ocean engineering and materials science.